Available online at www.joac.info

ISSN: 2278-1862

Journal of Applicable Chemistry
2018, 7 (6): 1534-1546
(International Peer Reviewed Journal)

A Green and Facile One-Pot Synthesis of Ag NPs using *Bombax Pendantrum* Leaf Extract for Effective Removal of Organic Dyes

Ramya Arumugam and Prakash Periakaruppan*

Department of Chemistry, Thiagarajar College, Madurai–625 009, Tamil Nadu, INDIA
Email: kmpprakash@gmail.com

Accepted on 28th September, 2018

ABSTRACT

Report a facile, green and one-pot synthesis of silver nanoparticles (Ag NPs) using Bombax Pendantrum leaf extract (BPLE) as both reducing and stabilizing agent. The synthesized Ag NPs was characterized by UV–Vis spectroscopy (UV-Vis), Infrared spectroscopy (IR), X-ray diffraction (XRD), Transmission electron microscopy (TEM) and tested for its ability to degrade the dyes such as RhB (Rhodamine B), NB (Nile Blue), MB (Methylene Blue), EB-T (Eriochrome Block T), MO (Methyl Orange), MG (Malachite Green), BG (Brilliant Green), BB (Bismerk Brown), RB (Rose Bengal), MR (Methyl Red). The green synthesized Ag NPs shows an excellent catalytic activity and the catalyst is very much able to be reused. The formation of Ag NPs and catalytic degradation of organic dyes are discussed.

Graphical Abstract

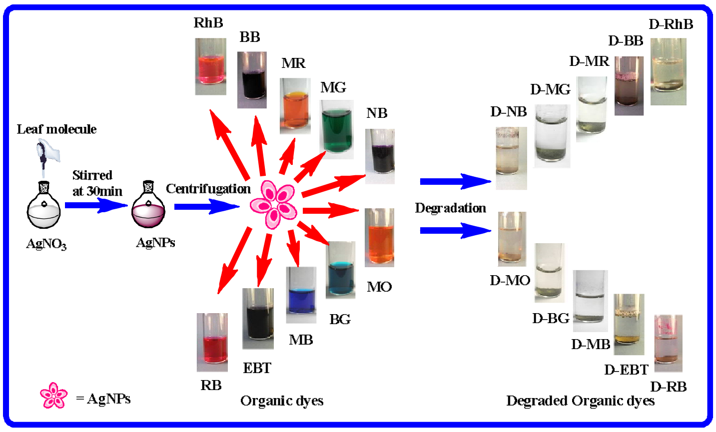

Synthesis of the Ag NPs using *Bombax pendantrum* Leaf extract and catalytic degradation of Organic Dyes.

Keywords: Green Synthesis, Ag NPs, Degradation, Organic Dyes, Reusability.

INTRODUCTION

The synthesis of metal nanoparticles with desired size and shape has, enormous importance, especially in the emerging field of nanotechnology. This high interest in nanoparticles is due to their unique optical [**1**], sensor [**2-4**], electronic and catalytic properties [**5**] with their distinctive feature of size and shape [**6, 7**]. Specifically, silver nanoparticles (Ag NPs) have attracted much attention over the last decade owing to their unique properties as compared to their bulk metal equivalents, including a large surface-to-volume ratio and tunable shapes [**8**]. Various synthetic routes for the preparation of monodisperse metal nanoparticles have been developed. Many of the existing physical and chemical methods suffer from a few drawbacks such as high cost, use of environmentally hazardous chemicals and non-availability of medical applications due to presence of toxic capping agents [**9, 10**]. These factors contributed towards exploration of new methods and materials for the production of nanoparticles based on the principles of ‘‘Green Chemistry’’ [**11**]. Biosynthesis of Ag NPs has gained much attention and emerged to be an active research area in the field of nanotechnology. There are numerous researches from both academia and industry that focus on both the synthesis and the applications of nanoparticles towards biological systems such as plants, marine algae, fungi and bacteria for the production of nanoparticles [**12-15**]. The compounds present in the biological systems can function as reducing as well as stabilizing agents and render more biocompatibility to biosynthesized nanoparticles [**16**]. These nanoparticles have been widely used in many fields such as biomedicine, electronics and chemistry [**17**]. A number of methods were used in the past for the synthesis of Ag NPs for example, co precipitation, deposition precipitation and chemical vapor deposition, reduction in solutions [18], thermal decomposition of silver compounds and recently via bio and green synthesis route [**19-21**]. Although metal nanoparticles are catalytically active, one major drawback of these particles is their tendency to agglomerate. To prevent aggregation, various approaches are pursued to stabilize nanoparticles. Here in this work the Ag NPs have been synthesized using *Bombax pendentrum* leaf extracts as reducing and stabilizing agents. Further, Green synthesis of Ag NPs from plant extracts is less expensive and can be used as an effective alternative for the production of metal nanoparticles on large-scale [**22-23**].

Various chemical industries such as paints, dyes, textiles, food, etc. have released hazardous dyes amalgamating with waste water. The presence of hazardous dyes in waste water can affect the aquatic plants because they reduce sunlight transmission through water. Dyes are also responsible for direct and indirect toxic effects on humans. Specifically, the exposition of humans to dyes has been linked to jaundice and tumor development, skin irritation, allergies, heart defects and mutations [**24-27**]. There are different types of dyes (natural dyes, synthetic dyes, azo dyes, etc.) are present in wastewater. Hence the removal of these hazardous pollutants from waste water is very imminent. Main advantages of Ag NPs are exploring simpler, lower cost and safer technologies are still needed for practical applications. Additionally, nanocatalysts can make the products easily removable from the reaction mixtures and make the recyclable catalysts [**28-30**].

In the present study, we have carried out a one-step synthesis of stable Ag NPs by using *BPLE* leaf extract as reducing as well as stabilizing agent with water as a solvent. Synthesized Ag NPs have been characterized by UV-Visible spectroscopy, FT-IR spectroscopy, XRD analysis, Zeta Potential analysis, HR-TEM and EDX analysis. The application of Ag NPs as a catalyst has been studied in the degradation of various dyes, including Rhodamine B (RhB), Nile Blue (NB), Methylene Blue (MB), Eriochrome Block –T (EB-T), Methyl Orange (MO), Malachite Green (MG), Brilliant Green (BG), Bismerk Brown (BB), Rose Bengal (RB), Methyl Red (MR) using $NaBH_4$ as a reducing agent. Besides, the Ag NPs have superior stability and recyclability.

MATERIALS AND METHODS

Chemicals: The silver nitrate ($AgNO_3$) and the dyes were purchased from Sigma–Aldrich, India and used as received. The *BPLE* was collected from Yadava College campus, Madurai, India. And all the other chemicals were also purchased from Sigma-Aldrich (Bangalore, India). Reagents were purely analytical grade and used without any further purification.

The Green Synthesis of Ag NPs: The Green synthesis of Ag NPs involves two major steps (Scheme 1); (i) Preparation of leaf extract from *Bombax pentandrum* and (ii) Synthesis of Ag NPs.

Preparation of Leaf Extract from *BP* leaves: The fresh *BP* leaves were cut into small pieces and washed with deionized water. This washing process was done several times to remove any unwanted dust and other contaminants. 25 mg of small pieces of *BP* leaves was taken in a 100 mL beaker and then added 50 mL of deionized water. The leaves were boiled at 90°C for 20 min and the extract was thrice filtered using Whatmann filter paper no. 1 to get clear solution. The filtered solution was pale yellow in color. And this leaf extract was used as reducing as well as stabilizing agent for the synthesis Ag NPs. The filtrate solution was stored in the refrigerator at 40°C for further use.

Synthesis of Ag NPs: The pale yellow colored *BPLE* solution (20 mL) was mixed with 20 mL of 1mM $AgNO_3$ solution. The color changed from pale yellow to deep brown color in 50 min and no further noticeable difference in the color of aqueous silver colloids was observed. It therefore indicates that the bio reduction process is over in 50 min. The green synthesized Ag NPs were collected by centrifugation and washed several times with deionized water. The dried Ag NPs were stored in a vial for further study.

Catalytic Degradation of Dyes: The catalytic activities of the prepared Ag NPs were investigated for the reduction of various dye solutions (such as RhB, NB, MB, EB-T, MO, MG, BG, BB, RB, MR) in the presence of the $NaBH_4$ and UV-Visible spectroscopy was used to follow the kinetics of catalytic reduction of dye solutions. In a typical kinetic experiment, 10 mL of dye solutions was dispersed with 40mL of the catalyst. About 1 mL of fresh $NaBH_4$ was added to the mixture suddenly (time lapse of 30 s). The solution was carefully mixed by shaking gently. The suspension was sampled at certain time intervals, filtered and UV-Visible spectra were recorded. Afterwards, the reaction was over, the mixture was centrifuged and washed with deionized water repeatedly to collect Ag NPs for reusability.

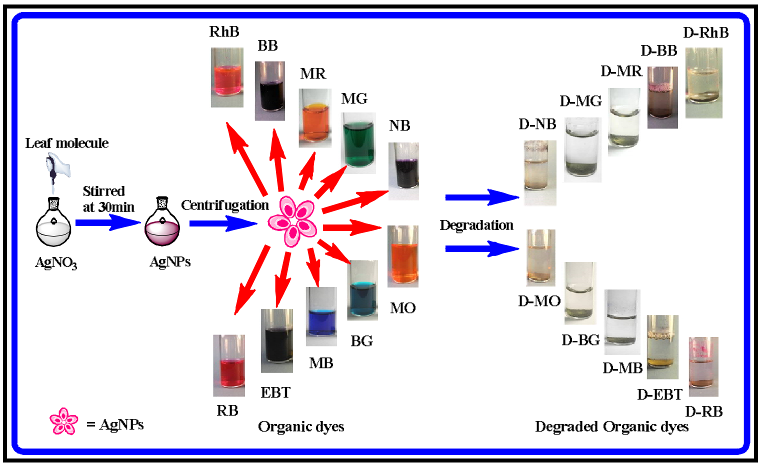

Scheme 1. Synthesis of the Ag NPs using *Bombax pendantrum* Leaf extract and catalytic degradation of Organic Dyes.

Characterization: The crystalline and its phases of the Ag NPs were analyzed by XRD 6000 with Cukα radiation (λ = 1.5412 Å) on JEOL JDX 8030 X- ray diffractometer. The functional group identification and composition was analyzed using a JASCO FT-IR 460 Plus spectrophotometer in the ranges from 4000–400 cm^{-1} (2.5-25 µm). The formation of Ag NPs was also confirmed by UV-Visible spectroscopy (JASCO V-530 Spectrophotometer). The sample measurements were performed in a 1 cm quartz cuvette at room temperature. Transmission electron microscopy (TEM) was performed with a JEOL JEM 2100 analytical scanning transmission electron microscope. The size and the morphology of the nanoparticles were determined by transmission electron microscopy. Energy Dispersive X-ray (EDX) analysis was performed to analyze size, shape, morphology, purity and elemental analysis of nanomaterials. Scheme. 1 Illustrates the formation mechanism of synthesized Ag NPs and catalytic degradation of organic dyes.

RESULTS AND DISCUSSION

UV-Visible Spectroscopy: The UV-Vis absorption spectra of synthesized Ag NPs obtained from the reaction of *BPLE* and $AgNO_3$ solution recorded in the range of 250 to 800 nm. The formation of Ag NPs was visually identified by means of a change in color of the reaction mixture from pale yellow to dark brown, depending on the intensity (Figure 1a). UV-visible absorbance spectral values at 440 nm confirm the bio reduction of silver ions to metallic silver (Figure 1b (curve a–f)) using the *BPLE*. The formation of the Ag NPs with different time intervals of 10, 20, 30, 40, 50 and 60 min indicates that there is no shift in the absorption peak position. Only the SPR intensity increases, which indicates the continuous reduction of the silver ions and the increase in the absorbance signifies the formation of Ag NPs. But here the absorption peak steadily increases and after 60 min there is no increase, which confirms that the reaction is completed within 60 min Figure 1c. The SPR absorbance peak is appeared (Figure 1d) same even after 24 h. Thus the formation of Ag NPs shows the higher stability. The observed SPR band at 440 nm is strong evidence for the successful formation of the Ag NPs.

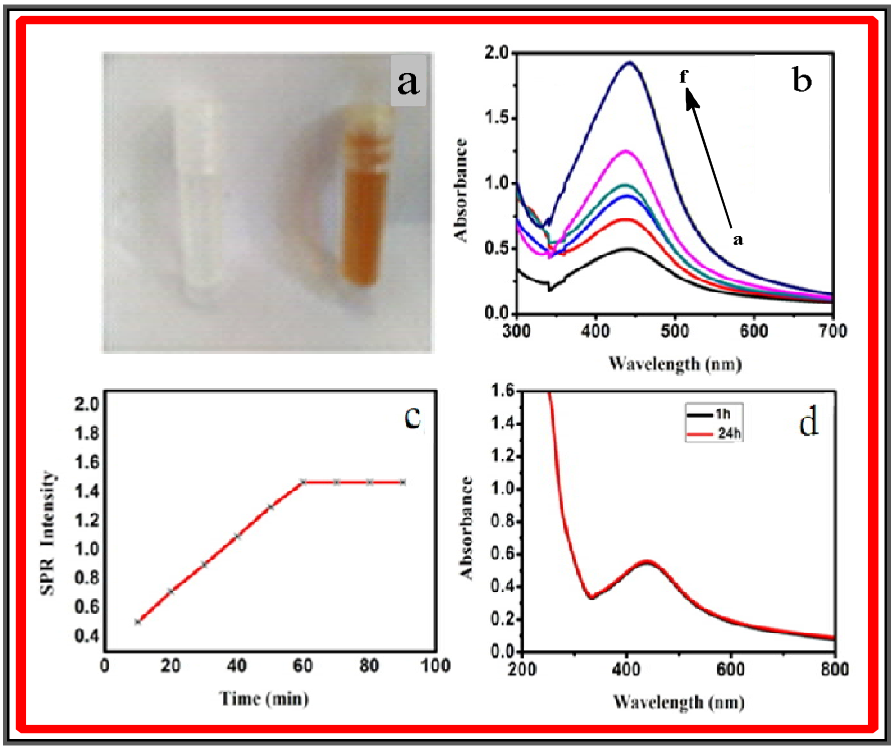

Figure 1. (a) shows photograph of change in color during the phytoreduction $AgNO_3$ to Ag NPs changes from light yellow to brown **(b)** UV-visible absorbance spectra of the Ag NPs as a function of time with a time interval of 10 min (curves a to f). **(c)** Plot of the intensity of the SPR peak at 440 nm against the reaction time. **(d)** UV-visible absorbance spectra of the Ag NPs after 60 min (black line) and after 24 h (red line).

FT-IR Spectroscopy: FT-IR measurements were carried out to find out the possible molecules present in the leaf extract of BP which are responsible for the reduction of the silver ions and the stabilization of the synthesized Ag NPs. The FTIR spectra of stable Ag NPs and *BPLE* are shown in figure 2. There are several characteristic peaks which appear in figure 2a. 1622 cm^{-1} is the C=O stretching vibration of the carbonyl and carboxylic group of amide I in the BP leaf proteins. The intense peak at 3409 cm^{-1} is due to the -OH stretching vibration of the hydroxyl functional groups of the polyphenols and alcohols and the -NH stretching vibrations of the amide(II) (or) amine. The sharp band at 2354 cm^{-1} was assigned to the vibrations of C–O–C in the constituents. The peaks at 2925 and 2850 cm^{-1} are characteristic of the stretching vibrations of methyl groups or the C=H stretching vibrations of aldehydic amine groups and the C–O stretching vibrations of the esters appear at 1731 cm^{-1}. The peaks observed at 1427 cm^{-1} are the bending vibration of the C–O–H groups and the peaks around 1236 cm^{-1} are the bending vibration of the C–N groups, amide II and III bands in the proteins. The peak appearing at 1152 cm^{-1} could be attributed to a carbonyl group as in the aldehydic and ketonic groups. The peak at 660 $cm^{-1}$is the plane bending vibration of the N–H groups in the proteins. The strength and intensity of all the peaks are obviously weakened. After reduction with the silver ions (Figure 2b) the strength of the peak at 3409 cm^{-1} represents the presence of proteins/ enzymes or polysaccharide components and is assigned to the vibration of the –N–N– groups. The stretching vibrations of the methyl groups or the C=H stretching vibrations of the aldehydic amine groups are observed at 2925 and 2850 cm^{-1} and the peak at 660 cm^{-1} indicates the reduction of the silver ions coupled to the oxidation of the amine components. Meanwhile the intensity of the above mentioned hydrogen bonded N–H groups weakens obviously. The observed results indicate the possible involvement of the above mentioned groups in the Ag NPs [31]. The peak at 1622 cm^{-1} is due to the C=O stretching vibration of the carbonyl and carboxylic groups present in the amide- I linkage of the proteins. As indicated by the FT-IR data, the plant extract contains phyto chemicals and functional groups like alcohol or phenol, amine, amide (I) and (II), aldehydes, polyol and methylene groups. Close observation of the shift and reduction in the intensity of the peaks from 1622 to 1640 cm^{-1} suggests that the amide-I linkage of the protein groups may be present on the surface of the Ag NPs [32-33]. This suggested that the Ag NPs were protected by the phytoconstituents of the *BPLE*.

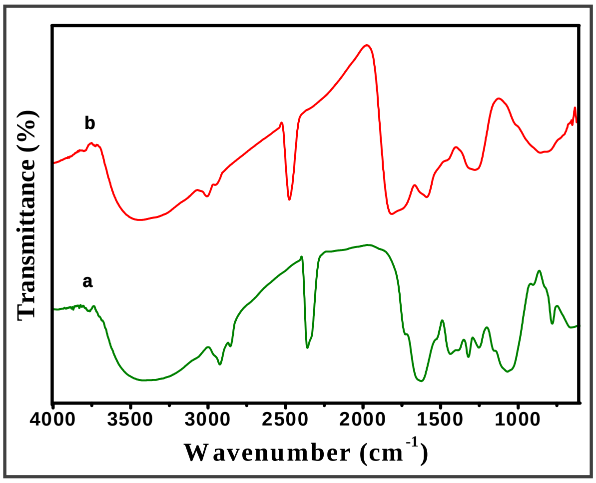

Figure 2. FT-IR spectral analysis of **(a)** BPLE and **(b)** Synthesized Ag NPs.

XRD Analysis: The crystalline nature of Ag NPs is confirmed by XRD analysis as shown in Figure 3. Characteristic formation of four different 2θ values of Ag NPs is at 38.1°, 44.3°, 64.4° and 77.4°. It can be attributed to (1 1 1), (2 0 0), (2 2 0) and (3 1 1) crystallographic planes of the face centered cubic (fcc) structure of Ag NPs and its positions and relative intensities of the peaks can be confirmed by JCPDS Card No.04-0783. From the signal patterns, it clears that the products are silver nanoparticles and well crystallized. The synthesized Ag NPs are essentially pure and the values of average crystalline size have been calculated using the Debye- Scherrer equation given below:

$$D= 0.9\lambda/\beta \cos\theta$$

Where, 0.9 is the shape factor, λ is the X-ray wavelength, β is the FWHM in radians and θ is the Bragg angle. The peak corresponding to (1 1 1) plane, more intense than other planes with predominant orientation and the synthesized Ag NPs, is crystalline in nature. The Scherrer formula were used to calculate the average size of the Ag NPs and found to be 22 nm correspond to (111) peak, obtained from the HR-TEM images.

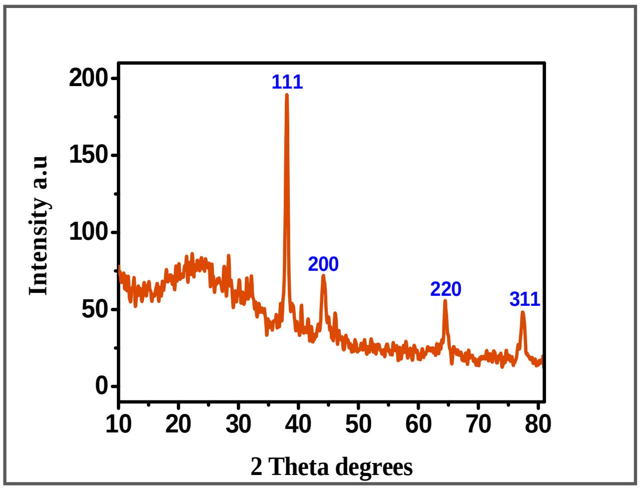

Figure 3. XRD pattern of synthesized Ag NPs from *BPLE.*

TEM: The surface morphology, size and shape of the Ag NPs were identified using HR-TEM images. Figure 4 (a-d) shows the HR-TEM images of different magnifications which confirms the presence of the Ag NPs. TEM images of the Ag NPs exhibit a typical spherical morphology. The approximate particle diameter was found to be in the range of 22 nm. Figure 5(a) shows EDX Spectrum which confirms the existence of Ag in the synthesized Ag NPs. The SAED pattern of synthesized Ag NPs is shown in figure 5(b). The presence of bright circular rings in the SAED patterns confirms the crystalline nature of Ag NPs. The spots corresponding to various orientations appearing inside the concentric rings also show that the obtained Ag NPs have a good crystallinity. Figure 5(c) shows the Frequency distribution of Histogram studies for finding the average particle size and calculated as 22 nm.

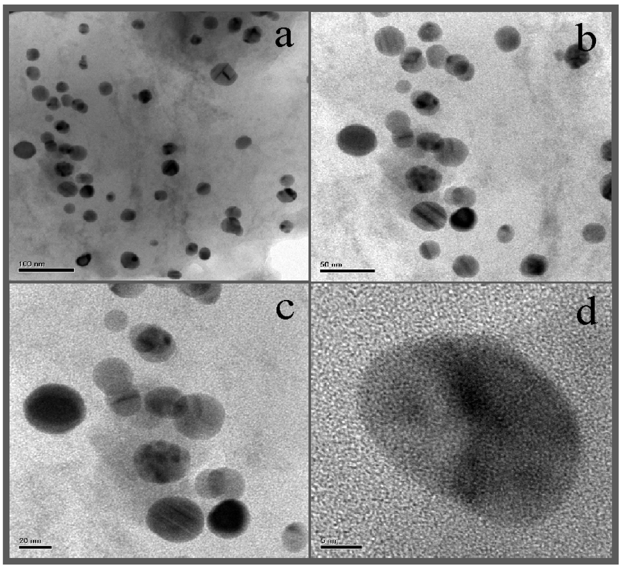

Figure 4. (a-d) HR-TEM images of different magnifications of synthesized Ag NPs.

Catalytic degradation of organic dyes: The catalytic degradation of organic dyes such as RhB, NB, MB, EB-T, MO, MG, BG, BB, RB, MR using $NaBH_4$ was used as reducing agent and carried out by the best catalytic activity of Ag NPs. In the absence of either Ag NPs or $NaBH_4$ no dedying process takes place. However, when Ag NPs used as a catalyst, the absorption intensity of organic dyes decreases successfully. Ag NPs effectively catalyzes the degradation of organic dyes by acting as an electronic relay system, wherein the electron transfer takes place from donor BH_4^- to acceptor dyes [34-36].

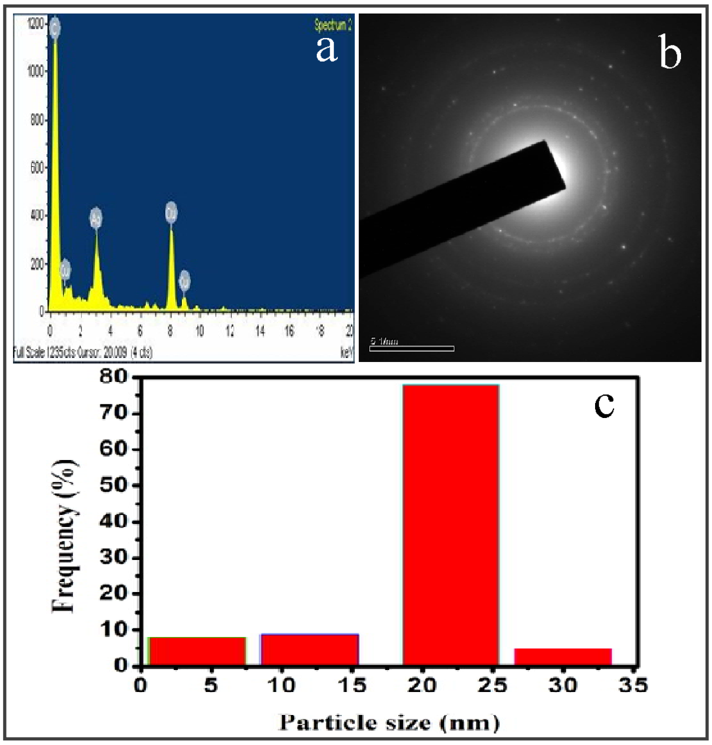

Figure 5. a) EDX spectrum of synthesized Ag NPs **b)** SAED pattern of Ag NPs **c)** Histogram for the particle size distribution of synthesized Ag NPs.

The degradation processes and kinetics can be monitored UV–visible spectrophotometrically. Figure 6 (a-j) shows that UV-Vis spectra of strong absorption peaks at 562, 620, 640, 539, 460, 619, 420, 450, 533, 426 nm corresponding to RhB, NB, MB, EB-T, MO, MG, BG, BB, RB, MR organic dyes respectively. In the absence of Ag NPs, there is no change in the absorption spectra, which indicates that there is no possible degradation by visible light. Among the various organic dyes used such as NB, MB, EBT, BB, RB, MR degraded 100%, 98%, 93.4%, 95%, 97.6% and 98% within 40, 80, 70, 80, 60, 60 sec. Furthermore, the percentage of degradation of MO (99%), MG (97%), RhB (100%) and BG (95%) takes place within 100 sec under light irradiation. The degradation of organic dyes and its kinetics are expressed as-

$$\mathrm{In}(C_0/C) = kt,$$

Where k is the observed rate constant (sec^{-1}) and C_0 and C (mg/L) are the concentrations of organic dyes and at time t, respectively. Figure 7 (a-b) shows that the ln (C/C_0) Vs time plots for kinetics rate constant for the degradation of organic dyes RhB, NB. Corresponding apparent reaction rate constants k were 9.03×10^{-3}, 5.23×10^{-3}, 4.26×10^{-3}, 6.51×10^{-3}, 3.78×10^{-3}, 4.81×10^{-3}, 4.72×10^{-3}, 8.014×10^{-3}, 9.03×10^{-3} and 7.53×10^{-3} for RhB, NB, MB, EBT, MO, MG, BG, BB, RB and MR respectively. An absorbance and a degradation efficiency of organic dyes (RhB, NB, MB, EB-T, MO, MG, BG, BB, RB, MR) and its rate constants k are tabulated in table 1.

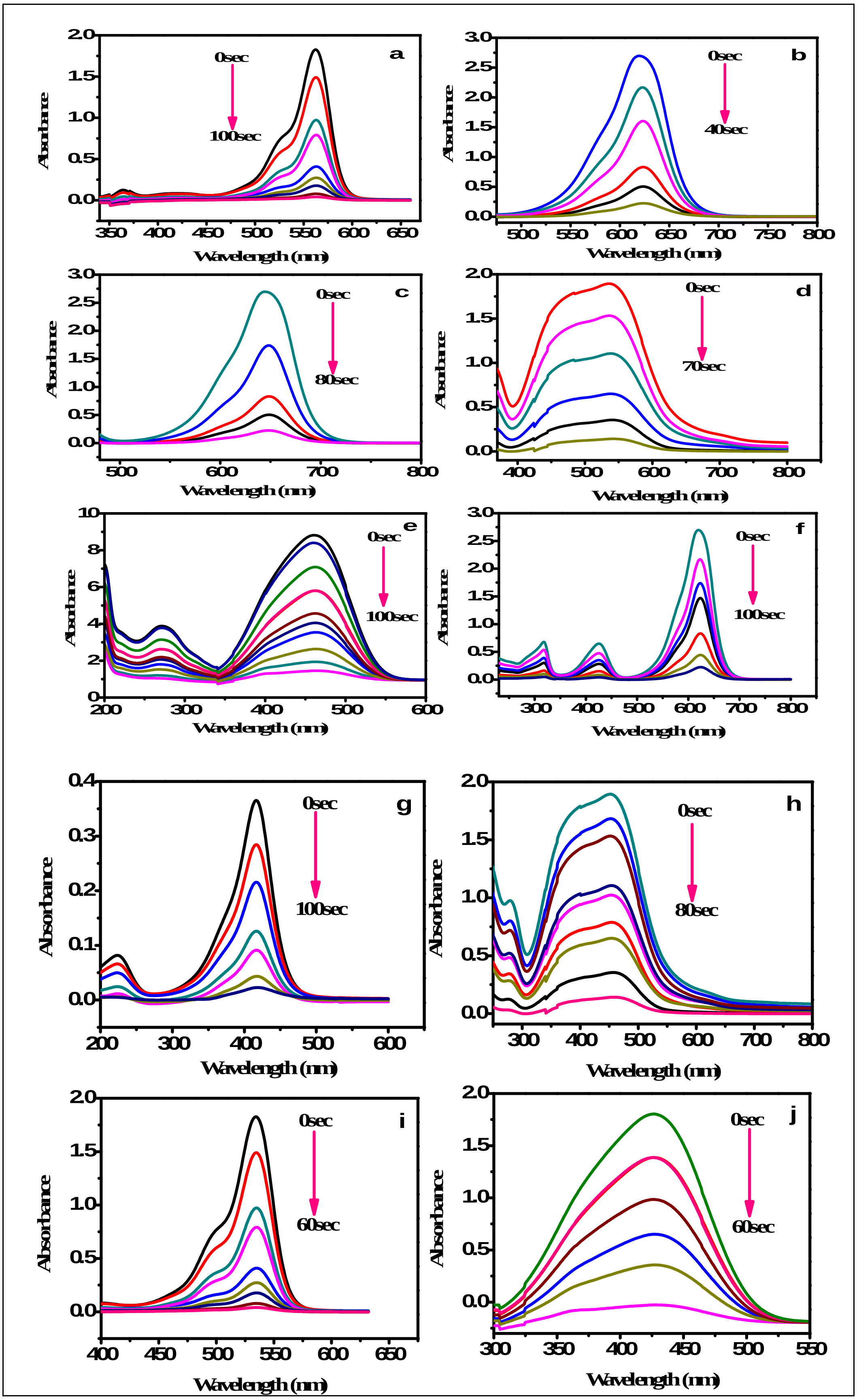

Figure 6(a-j). UV-visible spectra for the degradation of RhB, NB, MB, EB-T, MO, MG, BG, BB, RB, MR using $NaBH_4$ in the presence of Ag NPs.

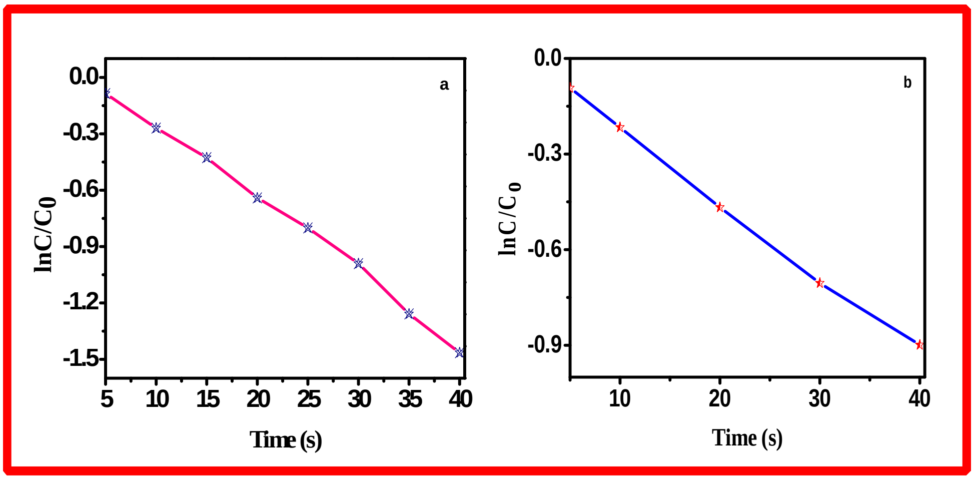

Figure 7. ln C/C_0 Vs time plots for kinetics rate constant for the degradation of organic dyes RhB, NB under UV irradiation.

Table 1. Comparison studies on the catalytic degradation of organic dyes using various metal nanomaterials BB (Bismerk Brown), BG (Brilliant Green), EB-T (Eriochrome Block T), MG (Malachite Green), MO (Methyl Orange), MB (Methylene Blue), NB (Nile Blue), RhB (Rhodamine B), RB (Rose Bengal), MR (Methyl Red).

Catalyst	**Size (nm)**	**Shape**	**Dyes**	**Degradation cycle**	**Degradation time**	**Efficiency %**	**Rate constant (K)**	**Ref**
Ag NPs	17	-	MO MB Ey	-	-	78	0.6626 1.0218 0.2312	[37]
Ag NPs	88	Spherical	MO	-	-	-	-	[38]
Ag_3PO_4-$CoFe_2O_4$ Nano composite	30	Core shell	MB RhB	-	60 min	7.5	-	[39]
Ag/RGO/TiO_2 nanocomposites	30	Thin film	CR MB	5	116sec	-	-	[40]
AuNPs	72.32 ± 21.80	Quasi-spherical	RhB	-	7min	50	12.7X10^{-3}	[41]
Au/PDMAEMA/RGO	-	Spherical	RB MO EY	5	30s 50s 60s	82 74 93	21.8x10^{-3} 26.2 8x10^{-3} 8.78x10^{-3}	[42]
Ag@AgI/ZnS microspheres	10–20	Micro spheres		5	-			[43]
Au/CeO_2-TiO_2	5	hemispherical shape	MB MO CR RhB MG	5	90min 90min 90min 10min 90min	100	122.2 x10^{-3} 1.2 x10^{-3} 1.95 x10^{-3} 8.9 x10^{-3} 3.39 x10^{-3}	[44]
PAAuNPs1 PAAuNPs2	28 ± 5.6 15.6±3.4	Spherical	MB EY MR CR EB	-	70 min 12. 5min 75min 60min 60min	-	-	[45]
Ag NPs	22	Spherical	BB BG EBT MG MO MB NB RhB RB MR	6	80sec 100sec 70sec 100sec 100sec 80sec 40sec 100sec 60sec 60sec	95 95 93.4 97 99 98 100 100 97.6 98	8.014x10^{-3} 4.72x10^{-3} 6.51x10^{-3} 4.81x10^{-3} 3.78x10^{-3} 5.23x10^{-3} 9.03x10^{-3} 9.03x10^{-3} 7.53x10^{-3}	This work

The recyclability: The recyclability of the Ag NPs catalyst was investigated and easily separated out even after the degradation reaction was completed and the process was repeated around six times. In this process, Ag NPs were recollected and it was sequentially washed using double distilled water and dried before reusing. The washed and dried Ag NPs were reused around six times for the catalytic degradation of dyes. Figure 8 shows the calculation of reducing potential of recollected and reused Ag NPs for RhB, NB, MB, EBT, MO, MG, BG, BB, RB and MR dyes. These processes were confirmed that the recollected and reused Ag NPs are highly active even after reusing six cycles. Thus, this work confirms the involvement of environmental safety purposes for all kinds of water based works against dye pollution.

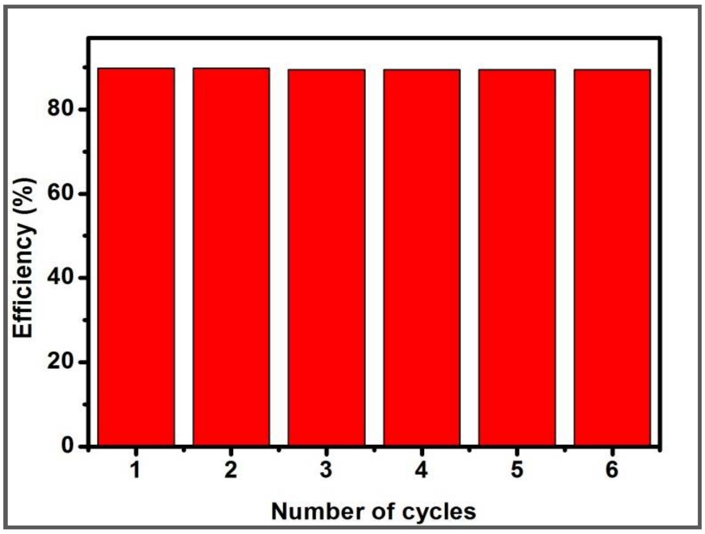

Figure 8. Recyclability of the Ag NPs catalyst

APPLICATION

One-pot green syntheses of silver nanoparticles are useful for the decontamination of organic dyes, reusability of the catalyst and excellent catalytic activity.

CONCLUSION

A simple and efficient way to synthesize stable and spherical Ag NPs using BPLE has been explained in detail in this report. The synthesized Ag NPs were initially confirmed by using UV-visible spectroscopy and TEM study. Through XRD studies, the crystalline nature of Ag NPs was evidenced and multifunctional nature of plant extract was confirmed by FTIR studies. Highly efficient catalytic degradation of toxic (RhB, NB, MB, EB-T, MO, MG, BG, BB, RB, MR) dyes has been demonstrated using Ag NPs catalyst which has excellent catalytic activity. The synthesized AgNPs effectively degrade the dyes with a removal yield as high as RhB (100%), NB (100%), MB (98%), EB-T (93.4%), MO (99%), MG (97%), BG (95%), BB (95%), RB (97.6%), MR (98%) in a short reaction time. The Ag NPs is small in size (22nm) with high surface area and spherical structure. Current report has suggested simple, cost effective and reusable and stable Ag NPs, which could be further used in analogous reactions and also in other experiments of environmental and industrial importance.

REFERENCES

[1]. C. N. Ramachandra Rao, G. U. Kulkarni, P. John Thomas, and P. P. Edwards, Metal nanoparticles and their assemblies, *Chem. Soc. Rev.*, **2000**, 29, 27-35.

[2]. M. Peng, L. Tao, X. Li, N. Limin, Y. Jian and H. Kun, Highly sensitive, label-free colorimetric assay of trypsin using silver nanoparticles, *Biosens. Bioelectron*, **2013**, 49, 20-24.

[3]. C. Morita-Imura, K. Zama, Y. Imura, T. Kawai, H. Shindo, Stimuli-responsive extraction and ambidextrous redispersion of zwitterionic amphiphile-capped silver nanoparticles, *Langmuir*, **2016**, 32, 6948- 6955.

[4]. E. A. Terenteva, V. V. Apyari, S. G. Dmitrienko, Y. A. Zolotov, Spectrophotometric determination of sulfates using silver nanoparticles stabilized with 6,6-ionene, *Chem. Bull.*, **2015**, 70, 157-161.

[5]. M. Maryami, M. Nasrollahzadeh, S. M. Sajadi, Green synthesis of the Pd/perlite nanocomposite using Euphorbia neriifolia L. leaf extract and evaluation of its catalytic activity, *Sep. Purif. Technol.*, **2017**, 184, 298-307.

[6]. N. Muthuchamy, A. Gopalan, K. P. Lee, A new facile strategy for higher loading of silver nanoparticles onto silica for efficient catalytic reduction of 4-nitrophenol, *RSC Adv.*, **2015**, 5, 76170-76181.

[7]. S. K. Das, E. Marsili, A green chemical approach for the synthesis of gold nanoparticles: characterization and mechanistic aspect, *Rev. Environ. Sci. Biotechnol*, **2010**, 9, 199-204.

[8]. J. M. Campelo, D. Luna, R. Luque, J. M. Marinas and A. A. Romero, Sustainable Preparation of Supported Metal Nanoparticles and Their Applications in Catalysis, *Chem Sus Chem.*, **2009**, 2, 18-45.

[9]. L. G. Wu, J. N. Shen, C. H. Du, T. Wang, Y. Teng and B. Van der Bruggen, Development of AgCl/poly (MMA-co-AM) hybrid pervaporation membranes containing AgCl nanoparticles through synthesis of ionic liquid microemulsions, *Sep. Purif. Technol.*, **2013**, 114, 117-125.

[10]. J. Fabrega, S. N. Luoma, C. R. Tyler, T. S. Galloway and J. R. Lead, Silver nanoparticles: behaviour and effects in the aquatic environment, *Environ. Int.*, **2011**, 37, 517–531.

[11]. J. A. Dahl, B. L. S. Maddux and J. E. Hutchison, Toward greener nanosynthesis, *Chem. Rev*, **2007**, 107, 2228-2269.

[12]. T. L. Doane and C. Burda, The unique role of nanoparticles in nanomedicine: imaging, drug delivery and therapy, *Chem. Soc. Rev.*, **2012**, 41, 2885-2911.

[13]. K. B. Narayanan and N. Sakthivel, Green synthesis of biogenic metal nanoparticles by terrestrial and aquatic phototrophic and heterotrophic eukaryotes and biocompatible agents, *Adv. Colloid Interface Sci.*, **2011**, 169, 59-79.

[14]. S. Sadhasivam, P. Shanmugam, M. Veerapandian, R. Subbiah and K. Yun, Biogenic synthesis of multidimensional gold nanoparticles assisted by Streptomyces hygroscopicus and its electro-chemical and antibacterial properties, *Biometals*, **2012**, 25, 351-360.

[15]. S. Ahmed, M. Ahmed, B. L. Swami and S. Ikram, A review on plants extract mediated synthesis of silver nanoparticles for antimicrobial applications: A green expertise, *Journal of Advanced Research*, **2016**, 7, 17-28.

[16]. F. Dumur, A. Guerlin, E. Dumas, D. Bertin, D. Gigmes, C. R. Mayer, Controlled spontaneous generation of gold nanoparticles assisted by dual reducing and capping agents, *Gold Bulletin*, **2011**, 44, 119-137.

[17]. I. Hussain, N. B. Singh, A. Singh, H. Singh, S. C. Singh, Green synthesis of nanoparticles and its potential application, *Biotechnol Lett.*, **2016**, 38, 545-560.

[18]. M. Annadhasan, T. Muthukumarasamyvel, V. R. Sankar Babu, N. Rajendiran, Green Synthesized Silver and Gold Nanoparticles for Colorimetric Detection of Hg^{2+}, Pb^{2+}, and Mn^{2+} in Aqueous Medium, *ACS Sustainable Chem. Eng*, **2014**, 2, 887-896.

[19]. A. Verma, M. S. Mahata, Controllable synthesis of silver nanoparticles using Neem leaves and their antimicrobial activity, *Journal of Radiation Research and Applied Sciences*, **2016**, 9, 109-115.

[20]. K. Tahir, S. Nazir, B. Li, A. U. Khan, Z. U. H. Khan, A. Ahmad, F. U. Khan, An efficient photo catalytic activity of green synthesized silver nanoparticles using Salvadora persica stem extract, *Sep. Purif. Technol.*, **2015**, 150, 316-324.

[21]. B. Ajitha, Y. Ashok kumar Reddy, P. Sreedhara Reddy, Green synthesis and characterization of silver nanoparticles using Lantana camara leaf extract, *Mater Sci Eng C Mater Biol Appl.*, **2015**, 49, 373-381.

[22]. V. Balakumar, P. Prakash, Silver-nanospheres as a green catalyst for the decontamination of hazardous pollutants, *RSC Adv.*, **2015**, 5, 105917-105924.

[23]. V. Ageetha, H. Soni, P. Padmaja Sudhakar, Palm shell extract capped silver nanoparticles -As efficient catalysts for degradation of dyes and as SERS substrates, *Journal of Molecular Liquids*, **2016**, 215, 787-794.

[24]. A. Luis, R. Montoya, V. Hernández-Montoya , A. Miguel, M. Moran, J. Jauregui-Rincon and J. F. Cervantes, Decolorization of dyes with different molecular properties using free and immobilized laccases from Trametes versicolor, *Journal of Molecular Liquids*, **2015**, 212, 30-37.

[25]. V. Mohammadtaghi, R. Mohd, S. Babak, A.Z. Abdullah, M.H. Ibrahim, K. B. Tan, Z. Gholami, P. Amouzgar, Application of chitosan and its derivatives as adsorbents for dye removal from water and wastewater: a review, *Carbohydr. Polym.*, **2014**, 113, 115-130.

[26]. M. Safdar, Y. Junejo, A. Balouch, Efficient degradation of organic dyes by heterogeneous cefdinir derived silver nanocatalyst, *Journal of Industrial and Engineering Chemistry*, **2015**, 31, 216-222.

[27]. H. Zouari-Mechichi, T. Mechichi, A. Dhouib, S. Sayadi, A. T. Martínez, M. J. Martínez, Laccase, purification and characterization from Trametes trogii isolated in Tunisia: decolorization of textile dyes by the purified enzyme, *Enzym. Microb. Technol.*, **2006**, 39, 141-148.

[28]. M.T. Yagub, T. K. Sen, S. Afroze and H. M. Ang, Dye and its removal from aqueous solution by adsorption: a review, Adv. Colloid Interf. Sci., **2014**, 209, 172-184.

[29]. B. Khodadadia, M. Bordbara, M. Nasrollahzadeha, Green Synthesis of Pd Nanoparticles at Apricot Kernel Shell Substrate Using Salvia Hydrangea Extract: Catalytic Activity for Reduction of Organic Dyes, *J Colloid Interface Sci.*, **2017**, 490, 1-10.

[30]. A. Rostami-Vartooni, M. Nasrollahzadeh, M. Alizadeh, green synthesis of seashell supported silver nanoparticles using bunium persicum seeds extract: application of the particles for catalytic reduction of organic dyes, *J Colloid Interface Sci.*, **2016**, 470, 268-75.

[31]. F. Dong, W. Guo, S.-K. Park, C.-S. Ha, Controlled synthesis of novel cyanopropyl polysilsesquioxane hollow spheres loaded with highly dispersed Au nanoparticles for catalytic applications, *Chem. Commun.*, **2012**, 48, 1108–1110.

[32]. J. Kasturi, S. Veerapandian, N. Rajendran, Biological synthesis of silver and gold nanoparticles using apiin as reducing agent, *Colloids Surf., B*, **2009**, 68, 55–60.

[33]. R. Emmanuel, K. Chelladurai, S.-M. Chen, P. Selvakumar, S. Padmavathy and P. Prakash, Green synthesis of gold nanoparticles for trace level detection of a hazardous pollutant (nitrobenzene) causing Methemoglobinaemia, *J. Hazard. Mater.*, **2014**, 279, 117–124.

[34]. T. Sinha, M. Ahmaruzzaman, High-value utilization of egg shell to synthesize Silver and Gold-Silver core shell nanoparticles and their application for the degradation of hazardous dyes from aqueous phase-A green approach, *J. Colloid and Interface Sci.*, **2015**, 453, 115-131.

[35]. V. S. Suvith, D. Philip, Catalytic degradation of methylene blue using biosynthesized gold and silver nanoparticles, *Spectrochim Acta Part A*, **2014**, 118, 526–532.

[36]. M. Safdar, Y. Junejo, A. Balouch. Efficient degradation of organic dyes by heterogeneous cefdinir derived silver nanocatalyst, *J. Ind. and Eng. Chem.*, **2015**, 31, 216-222.

[37]. V. K. Vidhu, D. Philip, Catalytic degradation of organic dyes using biosynthesized silver nanoparticles, *Micron*, **2014**, 56, 54-62.

[38]. T. Varadavenkatesan, R. Selvaraj, R. Vinayagam, Phyto-synthesis of silver nanoparticles from *Mussaenda erythrophylla* leaf extract and their application in catalytic degradation of methyl orange dye, *Journal of Molecular Liquids*, **2016**, 221, 1063-1070

[39]. L. Gan, L. Xu and K. Qian, Preparation of core-shell structured $CoFe_2O_4$ incorporated Ag_3PO_4 nanocomposites for photocatalytic degradation of organic dyes, materials and design, **2016**, 109, 354-360.

[40]. M. Nasrollahzadeh, M. Atarod, B. Jaleh, M. Gandomirouzbahani, *In situ* green synthesis of Ag nanoparticles on graphene oxide/TiO_2 nanocomposite and their catalytic activity for the reduction of 4-nitrophenol, congo red and methylene blue, *Ceramics International*, **2016**, 42, 8587-8596

[41]. A. Bhargava, N. Jain, M. A. Khan, V. Pareek, R. V. Dilip, J. Panwar, Utilizing metal tolerance potential of soil fungus for efficient synthesis of gold nanoparticles with superior catalytic activity for degradation of rhodamine B, *Journal of Environmental Management*, **2016**, 183, 22-32

[42]. N. K. Mogha, S. Gosain, T. D. Masram, Gold nanoworms immobilized graphene oxide polymer brush nanohybrid for catalytic degradation studies of organic dyes, *Applied Surface Science*, **2017**, 396, 1427-1434.

[43]. D. Amaranatha Reddy, J. Choi, S. Lee, T. K. Kim, Controlled synthesis of heterostructured Ag@AgI/ZnS microspheres with enhanced photocatalytic activity and selective separation of methylene blue from mixture dyes, *Journal of the Taiwan Institute of Chemical Engineers*, **2016**, 66, 200-209.

[44]. P. Saikia, A. T. Miah, P. P. DAS, Highly efficient catalytic reductive degradation of various organic dyes by Au/CeO_2-TiO_2 nano-hybrid, *Journal of Chemical Sciences*, **2017**, 129, 81-93.

[45]. R. Mata, A. Bhaskaran, S. R. Sadras, Green-synthesized gold nanoparticles from Plumeria alba flower extract to augment catalytic degradation of organic dyes and inhibit bacterial growth, *Particuology*, **2016**, 24, 78-86.